Tikrit Journal of Engineering Sciences (2025); 32(4): 2436
DOI: http://doi.org/10.25130/tjes.32.4.26

IRAQI Academic Scientific Journals

ISSN: 1813-162X (Print); 2312-7589 (Online)
Tikrit Journal of Engineering Sciences
available online at: http://www.tj-es.com

TJES Tikrit Journal of Engineering Sciences

Effect of Geometric Parameters on the Behavior of Concrete-Filled Steel Tubular Frames

Ali K. Al-Asadi *

Department of Civil Engineering, College of Engineering, University of Thi-qar, Thi-qar, Iraq.

Keywords:
Concrete-filled steel tubes; Composite structures; Frame ductility; Finite element analysis; Structural behavior.

Highlights:

- *The mixture of concrete with steel have many incredible benefits.*
- *Understanding the composite frame is the key in civil engineering field.*
- *The geometrical relationship between the various types of steel and the strength of the concert has positive impact on the solidity and the durability of buildings.*

ARTICLE INFO

Article history:

Received	29 Nov. 2024
Received in revised form	03 Dec. 2024
Accepted	07 Dec. 2024
Final Proofreading	27 Aug. 2025
Available online	30 Aug. 2025

Citation: Al-Asadi AK. **Effect of Geometric Parameters on the Behavior of Concrete-Filled Steel Tubular Frames**. *Tikrit Journal of Engineering Sciences* 2025; **32**(4): 2436.
http://doi.org/10.25130/tjes.32.4.26

Corresponding author:

Ali K. Al-Asadi
Department of Civil Engineering, College of Engineering, University of Thi-qar, Thi-qar, Iraq.

Abstract: Concrete-filled steel tubular (CFST) technology offers numerous structural benefits, including outstanding strength, fire resistance, and a considerable capacity for energy absorption. It has become crucial to investigate the ductility and stiffness of this type of structural system to gain an understanding of its capability to withstand external loads and prevent unexpected failure. This study provides insights into optimizing the design of CFST frames by offering a deeper understanding of how frame geometry affects their behavior. A finite element (FE) model was developed using specimen data from a previous study to analyze the behavior of the composite frame. The results of the FEA model were verified with the experimental data. An extensive analysis of the stress concentration in the CFST column, especially in the connecting portions, was conducted. Parametric studies were conducted to evaluate the impact of the axial load level, column length (L), and steel tube thickness (t) on the lateral stiffness and ductility behavior of CFST frames. For all frame models, no buckling occurred, and the failure mode was noticed after the formation of plastic hinges at the beam-column and base plate-column connections. The findings demonstrated that the lateral ductility of the CFST column improved with increasing L/D and D/t up to L/D equal to 15.53, at which point the development of lateral ductility was only slightly impacted by further increasing D/t. For all L/D ratios, the increase in skin thickness of the column tubes improved the stiffness of the frame; however, this improvement generally decreased noticeably as the L/D ratios increased. Increasing the length of the column with a small steel tube thickness (less than 2.67mm) insignificantly impacted the frame's ductility. On the other hand, increasing the column's length negatively impacted the frame's hardness in the case of a small steel tube thickness, i.e., less than 2.67mm.

تأثير المعلمات الهندسية على سلوك الإطارات الأنبوبية الفولاذية المملوءة بالخرسانة

علي كريم الاسدي
قسم الهندسة المدنية/ كلية الهندسة / جامعة ذي قار / الناصرية – العراق.

الخلاصة

تتمتع تقنية الأنابيب الفولاذية المملوءة بالخرسانة (CFST)بالعديد من المزايا الهيكلية، مثل القوة المتميزة ومقاومة الحريق والقدرة الكبيرة على امتصاص الطاقة. لقد أصبح من الضروري دراسة ليونة وصلابة هذا النوع من الأنظمة الإنشائية من أجل توفير فهم لقدرتها على تحمل الأحمال الخارجية ومنع حدوث أعطال غير متوقعة. تقدم هذه الدراسة رؤى حول تحسين تصميم إطارات CFST من خلال فهم أفضل لكيفية تأثير هندسة الإطار على السلوك. تم تطوير نموذج عناصر محدودة (FE)باستخدام بيانات عينة من دراسة سابقة لتحليل سلوك الإطار المركب. تم التحقق من نتائج نموذج FEA مع البيانات التجريبية. تم إجراء تحليل مكثف لتركيز الإجهاد في عمود CFST، خاصةً في الأجزاء الموصلة. أُجريت دراسات بارامترية لتقييم تأثير مستوى الحمل المحوري وطول العمود (Lوسُمك الأنبوب الفولاذي (tعلى الصلابة الجانبية وسلوك الليونة في إطارات القوالب الفولاذية المقاومة للتبريد. بالنسبة لجميع نماذج الإطار، لم يحدث أي التواء، ولوحظ وجود وضع فشل بعد تشكيل مفصلات بلاستيكية عند وصلات العمود-العارضة والعمود واللوحة الأساسية-العمود. أظهرت النتائج أن الليونة الجانبية لعمود القالب القابل للتفتيت الجانبي تحسنت مع زيادة L/D وD/t حتى L/D يساوي ١٥,٥٣، وعند هذه النقطة لم يتأثر تطور الليونة الجانبية إلا بشكل طفيف بزيادة نسبة L/D. بالنسبة لجميع نسب L/D، أدت زيادة سُمك جلد أنابيب العمود إلى تحسين صلابة الإطار؛ ومع ذلك، انخفض هذا التحسن بشكل عام بشكل ملحوظ مع زيادة نسب L/D، حيث لم يكن لزيادة طول العمود مع سُمك أنبوب فولاذي صغير (أقل من ٢,٦٧ مم) أي تأثيرات كبيرة على ليونة الإطار. من ناحية أخرى، كان لزيادة طول العمود تأثير سلبي على صلابة الإطار في حالة سمك الأنبوب الفولاذي الصغير (أقل من ٢,٦٧ مم).

الكلمات الدالة: الأنابيب الفولاذية المملوءة بالخرسانة، الهياكل المركبة، ليونة الإطار، تحليل العناصر المحدودة، السلوك الإنشائي.

1.INTRODUCTION

Due to their high strength, rigidity, and ductility, CFST has been used in constructions subject to static and dynamic side loads. Several studies have been conducted to assess the structural behavior of CFST frames using various parameters. Shams and Saadeghvaziri [1] discussed the effect of steel tube wall thickness on composite frame response in a state-of-the-art work on tubular CFSTs. Zhao and Grzebieta investigated square hollow beams filled with different types of concrete under seismic loads. Other researchers have indicated that circular tubes provide post-yield stiffness and strength that are significantly higher than those of most square or rectangular cross-sections [2]. Hu et al. investigated the influence of the steel tube shape and diameter-to-thickness ratio on the behavior of CFST frames [3]. Han et al. studied the response of the CFST column to torsion. The finite element (FE) method and the ABOCUS (software program) were used in this study to simulate the CFST column model. Han et al. utilized ABAQUS software to simulate CFST frames with a steel beam [3, 4]. FE models were employed to predict the structural behavior of composite frames subjected to cyclic loads. Han et al. studied the structural behavior of CFST frames composed of CFST steel beam columns under vertical static load and lateral cyclic forces [5]. Ding et al. evaluated the structural behavior of the CFST frame under axial and lateral seismic force [6]. Ahmed and Guenyisi investigated the effects of steel tube thickness, beam-column stiffness ratio, slenderness ratio, and infilled concrete types on the lateral carrying capacity of CFST and CFDST frames [7, 8]. It is noted that all previous studies available have focused on evaluating the behavior of such structures under dynamic loads. However, few studies have investigated the behavior of this type of frame under the influence of the lateral static load to which buildings are typically exposed. The goal of the present study is to evaluate the ductility behavior and the corresponding stiffness of circular CFST frames composed of CFST columns connected to an I-steel beam and loaded with constant axial and gradually increasing lateral loads. FE models using the ANSYS program were simulated to determine the structural response of the CFST frames [9]. The design parameters of most international codes are the height-to-diameter (L/D) and diameter-to-skin thickness (D/t) ratios of the CFST [10, 11]. The mentioned parameters and their impact on the ductility and stiffness of the whole frame were investigated. Also, statistical analysis was conducted. Generally, the study provides insights into optimizing the design of CFST frames by offering a deeper understanding of how frame geometry influences their behavior. The authors' previously published paper studied the concrete properties in depth [12].

2.EXPERIMENTAL PROGRAM

2.1.Apparatus and Procedures

CFST FRAMES MODELED IN THE ANALYSIS

Table 1 illustrates the details of nine CFST connected to a steel beam. Material properties were concrete strength of 42.6 MPa and steel yield stress of 352 MPa, as considered by Han et al. [5, 13] as a reference specimen. Figure 1 illustrates composite frame views and views of the beam-column connection and column-base connection. The length of the beam was 2500 mm with a section of (140×65×3.44×3.44) mm [7].

Table 1 Details of the CFST Frame.

item	Specimen section (mm)	Length (mm)	D/t	L/D	N_o kN
F_{1-1}	ColumnΦ140×3.34 Beam140×65×3.4×3.4	1450 2500	41.9	10.35	655
F_{1-2}	ColumnΦ140×2.67 Beam140×65×3.4×3.4	1450 2500	52.4	10.35	607
F_{1-3}	ColumnΦ140×2.00 Beam140×65×3.4×3.4	1450 2500	70.0	10.35	566
F_{2-1}	ColumnΦ140 ×3.34 Beam140×65×3.4×3.4	2175 2500	41.9	15.53	655
F_{2-2}	ColumnΦ140 ×2.67 Beam140×65×3.4×3.4	2175 2500	52.4	15.53	607
F_{2-3}	ColumnΦ140 ×2.00 Beam140×65×3.4×3.4	2175 2500	70.0	15.53	566
F_{3-1}	ColumnΦ140 ×3.34 Beam140×65×3.4×3.4	2900 2500	41.9	20.71	655
F_{3-2}	ColumnΦ140 ×2.67 Beam140×65×3.4×3.4	2900 2500	52.4	20.71	607
F_{3-3}	ColumnΦ140 ×2.00 Beam140×65×3.4×3.4	2900 2500	70.0	20.71	566

*No, axial load capacity of the CFST column.

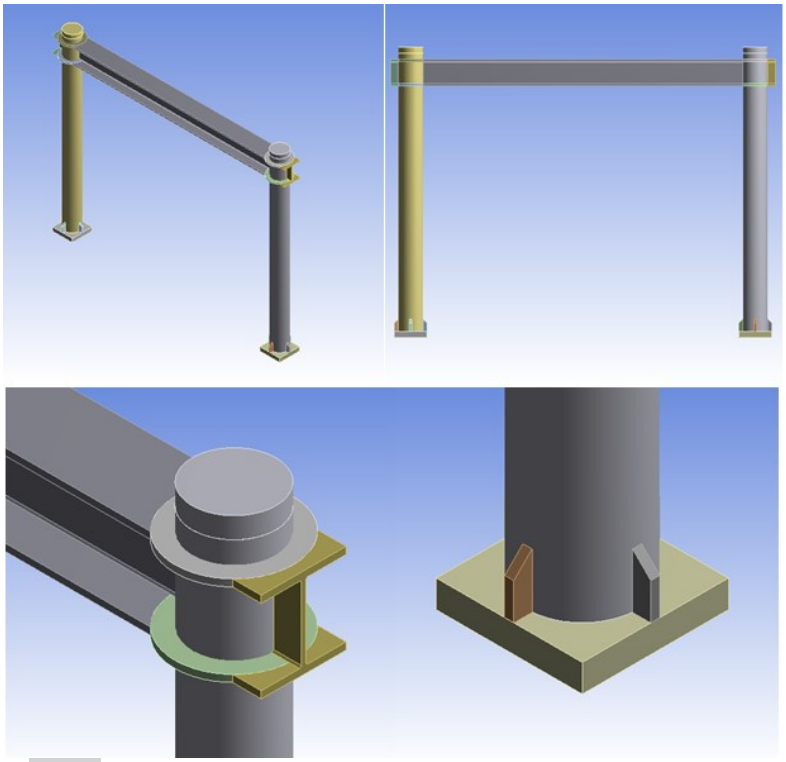

Fig. 1 Frame Structure with CFST Columns and Steel I-Beam.

3. MODELLING

Finite Element (FE) modelling using ANSYS was conducted. Using Element (Solid 186), the circular steel casing, the steel beam, and its reinforcing ribs were all modeled. The element had 20 nodes, three degrees of freedom at each node, translation in the x, y, and z nodal directions, and may, therefore, be deformed plastically. A 40.0 mm thick steel baseplate and top plate on the end of the column, modelled using element (Solid 185), were added to the fixed support places for the CFST to prevent stress concentration problems. This addition made it possible for the stress to be distributed more evenly throughout the support location. The element was capable of plastic deformations, cracking, and crushing in all three directions. It was identified utilizing eight nodes, each with three degrees of freedom, and translation in the x, y, and z nodal directions. Different mesh sizes were tested to find the best one (25mm) in terms of result stability and time consumption. Typical meshes of the composite frames are shown in Fig. 2. At the interface between the steel shell and concrete core, a friction coefficient of 0.6 was used. The concrete elastic modulus and Poisson's ratio used were 33800 MPa and 0.2, respectively, for the simulated frames. ANSYS software allows for bilinear or multilinear stress-strain curves for steel. The elastic stages, up to the proportional limit, were modeled using the elasticity modulus of the steel tube and beam, which were 20.066 and 20.016 GPa, respectively, and a Poisson's ratio of 0.262.

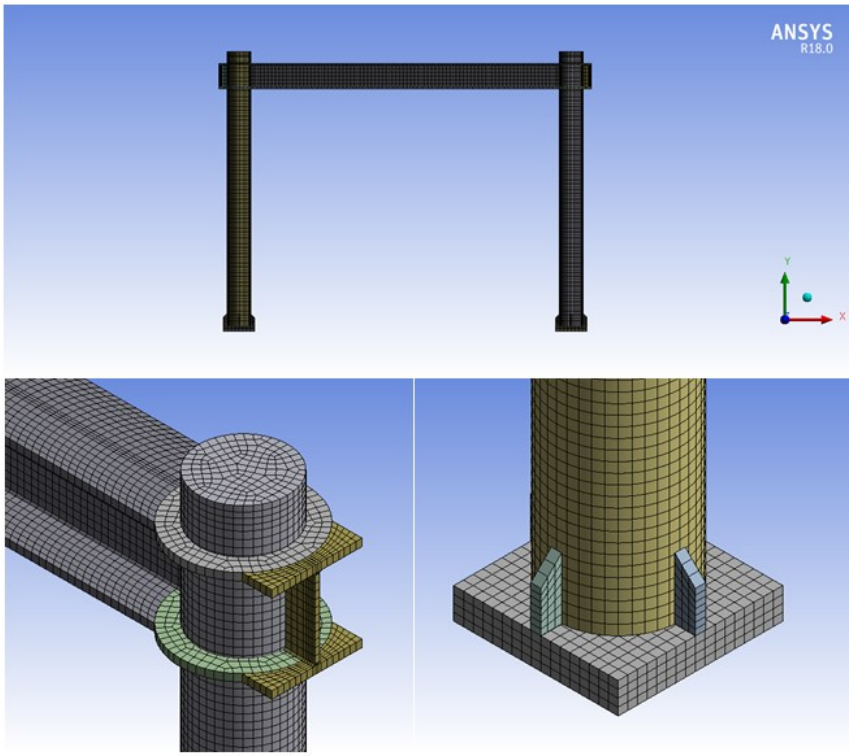

Fig. 2 Mesh Distribution for the Composite Frame.

4.MATERIAL PROPERTIES

The material properties of the CFST frames are

4.1.Concrete

The uniaxial behavior of the steel tube is modeled using an elastoplastic simulation [14]. The comparable uniaxial stress-strain curves for both unconfined and confined concrete are shown in Fig. 3, where f'_c is the compressive strength of the unconfined concrete cylinder. Eqs. (1) and (2) can be used to get the confined concrete compressive strength (f'_{cc}) and the related confined strain (ε'_{cc}), with the corresponding unconfined strain (ε'_c) being assumed to be 0.003 [15].

$$f'_{cc} = f'_c + k_1 f_l \quad (1)$$

$$\varepsilon'_{cc} = \varepsilon'_c \left(1 + k_2 \frac{f_l}{f'_c}\right) \quad (2)$$

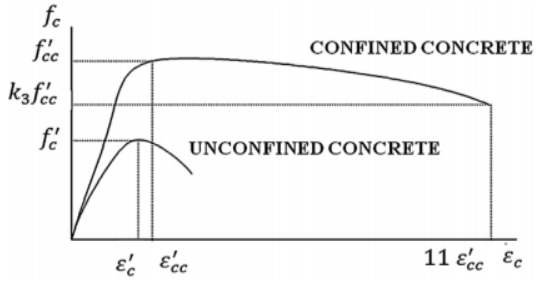

Fig. 3 Uniaxial Stress–Strain Relationships for Confined and Unconfined Concretes [14].

k_1 and k_2 (confinement coefficients) are fixed and can be determined experimentally. Constants k_1 and k_2 were determined to be 4.1 and 20.5, as reported by Richart et al., where f_l represents the lateral confining pressures around the concrete core, computed using the following empirical Eqs. (3a) and (3b) for CFST columns with circular section [15, 16]:

$$f_l = 0.043646 - 0.000832\left(D/t\right),\ 21.7 < D/t > 47 \quad (3a)$$

$$f_l = 0.006241 - 0.0000375\left(D/t\right),\ 47 < D/t > 150 \quad (3b)$$

The stress after the yielding can be obtained by:

$$\sigma = \frac{E_{cc}\,\varepsilon}{1+(R+R_E-2)\left(\frac{\varepsilon'_c}{\varepsilon'_{cc}}\right)-(2R-1)\left(\frac{\varepsilon'_c}{\varepsilon'_{cc}}\right)^2+R\left(\frac{\varepsilon'_c}{\varepsilon'_{cc}}\right)^3} \quad (4)$$

Where E_{cc}, R_E, and R could be computed from

$$E_{cc} = 4700\left(\sqrt{f_{cc}}\right) \quad (5)$$

$$R_E = \frac{E_{cc}\varepsilon'_{cc}}{f'_{cc}} \quad (6)$$

$$R = \frac{R_E\ (R_\sigma - 1)}{(R_\varepsilon - 1)} - \frac{1}{R_\varepsilon} \quad (7)$$

where R_σ and R_ε equal 4, as assumed by [16]. The final point of the curve is $k_3 f'_{cc}$ and ε'_{cc}. The coefficient k_3 (Material degradation parameter) could be calculated from [14]:

$$k_3 = 1\ ,\ 21.7 < D/t > \ 47 \quad (8)$$

$$k_3 = 0.0000339\left(D/t\right)^2 - 0.010085\left(D/t\right) + 1.3491 \quad (9)$$
$$47 < D/t > \ 150$$

It can be shown that as the D/t ratio rises, the lateral confining pressure f_l and the material degradation parameter k_3 drop. Due to the lateral restriction caused by the steel tube, f_l and k_3 tend to be high when the D/t ratio is low. The lack of lateral support from the tube causes f_l and k_3 to typically be modest when the D/t ratio is high.

4.2.Steel Tubular Columns and Base Plate

Stress-stain curves obtained from tensile tests provide the basis for tensile stress-strain relationships for steel in the FE mode rules. Figure 4 depicts the actual stress-strain curves

for the tube steel and beam steel. The negative slope regions of the stress-strain curve for tube and beam steel were removed to develop the convergence of the FE model. After the yield, the $0.01E_s$ slope part was considerably modified to a slope suitable for analysis [10].

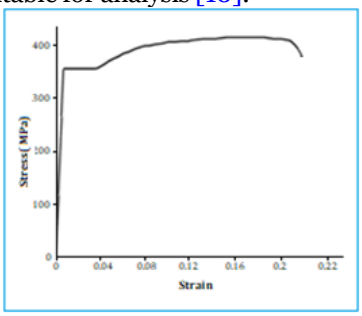

(a) Tube steel.

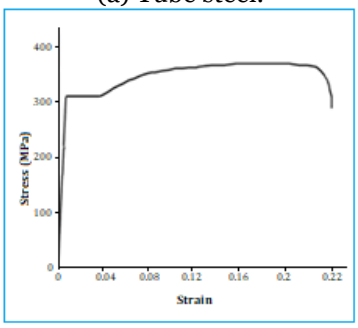

(b) Beam steel.

Fig. 4 Tensile Stress-Strain Curve for (a) Tube Steel, (b) Beam Steel.

5.VERIFICATION OF THE FE MODEL

For verification of the validity of the FE model, the FE models' results were compared to the experimental ones. The experimental composite frames composed of circular CFST columns and steel beams, studied by Han et al., were simulated in the present paper for verification of the FE models using the ANSYS software [5]. The following are the basic details for the frame (CF-23): The height of the CFST column (H) was 1450.00 mm, the span of the steel beam (L) was 2500.00 mm, the diameter of the CFST column was Φ140.00, and the thickness of the steel tube was 3.34 mm. The depth of the steel beam (h) × width of the flange (b_f)× thickness of the flange (t_f)× thickness of the web (t_w) were 140.00×65.00×3.44×3.44 mm, respectively. The structural properties of CFST columns and beams are illustrated in Table 2. Verification results are illustrated in Table 3. Figure 5 shows the shape of a deflected simulated frame by ANSYS software. Figure 6 illustrates the maximum principal normal and shear stresses at the frame connection. From the comparison, it can be figured out that accurate results were achieved for the FE simulation to predict the lateral ultimate load and lateral displacement of the composite frames, as shown in Table 3.

Table 2 The Material Properties of CFST Frames [7].

Element	Yielding Stress f_y (MPa)	Ultimate Stress f_u (MPa)	Elasticity Modulus (MPa)	Poisson's Ratio υ
CFST Column	352.0	430.1	2.066×10^5	0.262
Steel Beam	303.0	440.9	2.061×10^5	0.262

Table 3 The Verified Theoretical and Experimental Results.

Item	The experimental results of Han et al. (2011)"	The theoretical FE model results	$\frac{\text{Theoretical}}{\text{Experimental}}$ %
Ultimate lateral load (kN) (Ultimate Frame Capacity)	75.66	76.12	100.6
Lateral displacement of the frame at yield (mm)	14.72	14.66	99.6

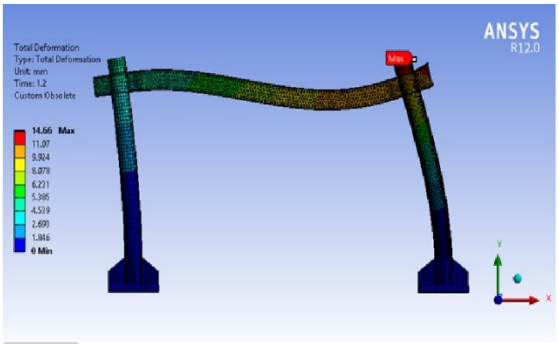

Fig. 5 The Shape of Deflected Modeled Frame.

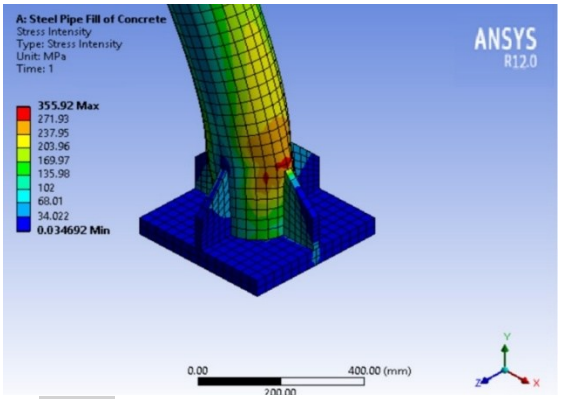

Fig. 6 Max Principal Stresses at the Base Connections.

6.ANALYSIS TYPE AND BOUNDARY CONDITION

The FE models were analyzed using the static method. The loads applied to the frame models were divided into many steps of load increments in the nonlinear analysis. Upon completing each incremental solution, the stiffness matrix of the model was modified to reflect the nonlinear change in frame stiffness before proceeding to the next force increment. ANSYS software (2016) utilizes the Newton-Raphson equation iteration to update the stiffness of the modeled frame. The Newton-Raphson equation produces convergence at the end of each force, increasing within the tolerances.

7.FAILURE MODES

Figures 7 and 8 show the failure mode and maximum stress obtained from the FE models. CFST frames showed the same collapse modes. Plastic hinges were installed on the bottom and top of the CFST. No core concrete crushing was noticed. Therefore, compound actions were maintained throughout the process.

8.MAX STRESSE

Maximum stress contours were illustrated in Figs. 7 and 8. Maximum stresses were found at the column-beam with a value of 381.46 MPa. The maximum value was observed at the beam-column connections and at the top and bottom of the CFST column. Both maximum values, 81.46 and 386.63 MPa (>352 MPa), indicate that the plastic hinge formations were located at the base plates and beam-column joints. Figure 9 shows the shape of the deformed CFST frame.

9.LOAD DISPLACEMENT RESPONSE

Figure 10 shows the lateral load-displacement relationships for CFST with lengths of L = 1450 mm, 2175 mm, and 2900 mm, each corresponding to steel tube thicknesses of t = 3.34 mm, 2.67 mm, and 2.00 mm, respectively. Table 4 illustrates the lateral load at yielding and failure strength, and related lateral displacement, for the CFST frames. It should be noted that P_y and Δ_y are yielding forces and related lateral movement at yield. P_u and Δ_u are the final load and related lateral movement at the instance of the ultimate load of the frame.

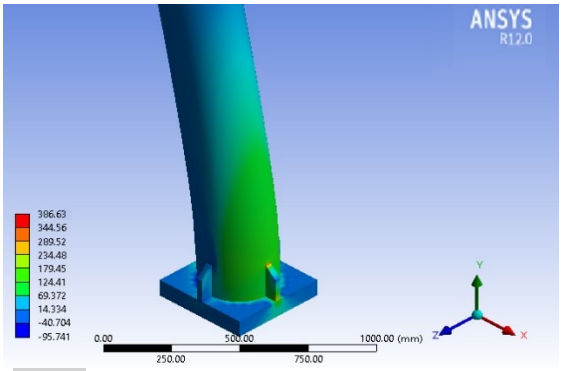

Fig. 7 Failure Modes and Max Stress at CFST Column-Base Plate Connection.

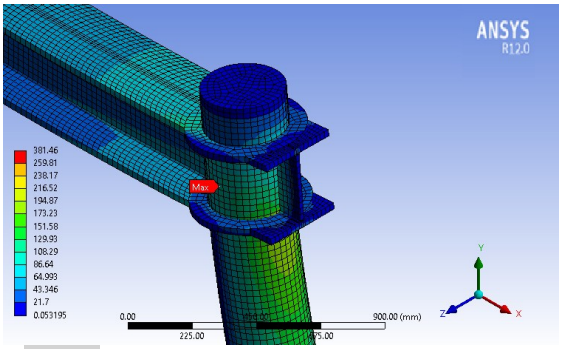

Fig. 8 Maximum Stresses at Beam-Column Connection.

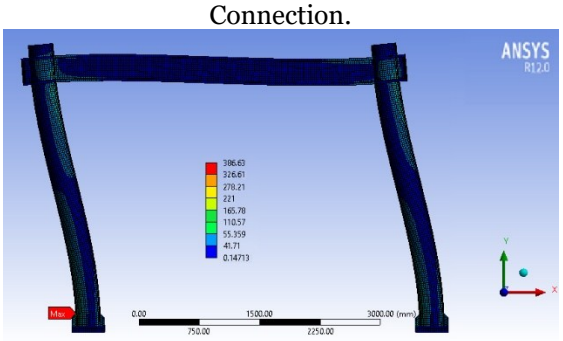

Fig. 9 Shape of the Deformed CFST Frame.

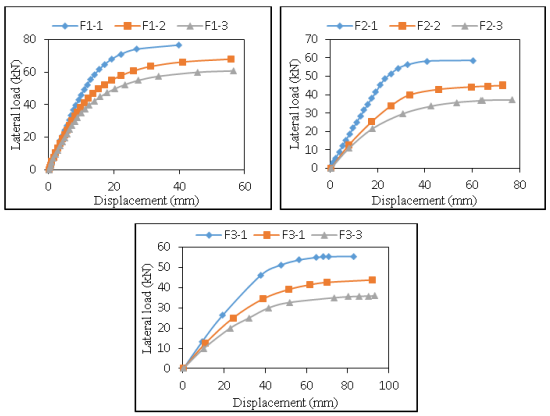

Fig. 10 Lateral Load–Lateral Displacement Curves for CFST Various Lengths and Various Steel Tube Thicknesses.

Table 4 Yield and Ultimate Lateral Force and Corresponding Displacements for the Composite Frames.

Frame	L (mm)	T (mm)	Δ_y (mm)	P_y (kN)	Δ_u (mm)	P_u (kN)
F1-1	1450	3.34	14.6	59.20	39.88	76.12
F1-2	1450	2.67	10.0	46.02	55.73	63.96
F1-3	1450	2.00	7.2	27.09	56.45	60.69
F2-1	2175	3.34	19.3	41.31	60.42	58.66
F2-2	2175	2.67	17.4	25.20	72.90	45.00
F2-3	2175	2.00	12.2	16.24	76.66	37.11
F3-1	2900	3.34	24.3	38.50	82.87	55.34
F3-2	2900	2.67	22.6	23.72	91.90	43.75
F3-3	2900	2.00	20.7	15.65	93.15	35.87

Considerable margins can be observed between Pu and Py, as well as between Δu and Δy. The difference is greater for the smaller-column-size frames. The lateral load capacity decreased with decreasing steel tube thickness and increasing height of the CFST column. It could be figured out that CFST frames with steel tubes of t = 3.34 mm resist better and stiffer behavior compared to others (different thickness). At the height of L = 1450 mm, the ratio of CFST frames with steel tube thickness of t = 3.34 mm, strength to CFST of t = 2.67 mm, and t = 2.00 mm at ultimate strength was 76.12 kN /63.96kN = 1.19, and 76.12 kN / 60.69kN =1.25. The effects of the height of columns are evaluated as well. It could be found that the strength of CFST frames with steel tube t = 3.34 mm and length L = 1450 mm, to CFST frames with L = 2175 mm and L = 2900 mm at ultimate strength were 76.12 kN /58.66kN = 1.30, and 76.12 kN / 55.34kN = 1.40.

10.DISPLACEMENT DUCTILITY

Figure 10 shows the values of frame displacements, which indicate the ductility of the frames. An increase in ductility of frames with increasing column height and also with decreasing column tube thickness was obtained, which is shown clearly in Fig. 11. Also, it is noticed that with increasing slenderness ratios of the column, the effect of tube thickness becomes less on ductility. Table 5 illustrates the displacements (Δ_u/Δ_y) ratio for CFST frames. The ductility ratio ranged from 2.72 to 7.79, indicating good ductility of the composite frames. It can be noted that the CFST frames were exposed to axial forces that affected the value of lateral force, resulting in less lateral movement at failure.

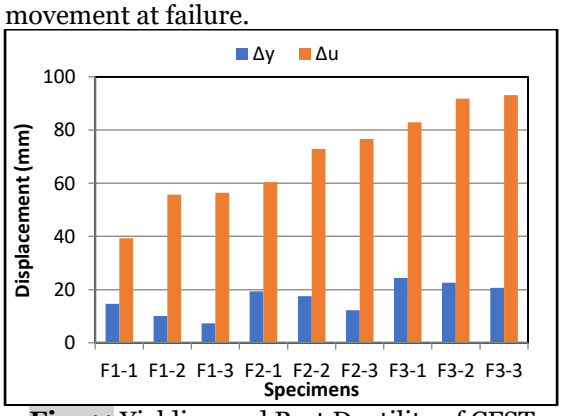

Fig. 11 Yielding and Post Ductility of CFST Frames.

11.STIFFNESS

Stiffness is one of the most important features that any structural part must possess, representing the ability of the structure to resist deflection due to the applied force. After the elastic range of any structure, the stiffness begins to decrease dramatically, shown through the load-deflection curve. Therefore, a complete perception of this situation must be available. In this study, the primary stiffness was calculated as the slope of the straight part of the lateral load-lateral displacement curve. The results showed that the stiffness increased with the thickness of the steel tube of the column, as well as the decrease in the length of the CFST column. Generally, the stiffness was observed in the first three specimens, i.e., F1-3, F1-2, and F1-1, where the thickness increased from 2.00mm to 3.34mm, showing a notable improvement from 3 kN/mm to 4.3 kN/mm. Additionally, the lateral stiffness of the F2-1 and F3-1 cases was 1.6 kN/mm and 1.5 kN/mm, respectively, as shown in Table 6.

Table 5 Displacement Ratio (Δu/Δy) for CFST Frames.

Frame	Δ_u/Δ_y
F1-1	2.72
F1-2	5.54
F1-3	7.79
F2-1	3.13
F2-2	4.17
F2-3	6.26
F3-1	3.40
F3-2	4.06
F3-3	4.45

Table 6 Stiffness for CFST Frames.

Frame	Stiffness (kN/mm)
F1-1	4.3
F1-2	3.3
F1-3	3.0
F2-1	1.6
F2-2	1.1
F2-3	1.0
F3-1	1.5
F3-2	1.1
F3-3	1.1

12.STATISTICAL ANALYSIS

Statistical analysis was employed to evaluate the results obtained through various changes in the materials specifications. MATLAB was employed to obtain the results. According to statisticians, the most valuable value through which engineers can understand what is happening to us is the p-value, as it was used in

the authors' previous paper ([2]). This value (p-value) represents the extent to which the significant parameter influences the other variable, which is statistically referred to as the independent variable. When the value of the p-value is less than 0.05, it means that the effect of the parameter is significant, and if the value is more than 0.05, the effect of this parameter is insignificant. By examining the resulting p-value, the trend path can be determined. In this statistical study, the change in the thickness and length of the tube forming the column were considered as independent variables, and ductility and stiffness were considered as dependent parameters. The p-value values were obtained using the Minitab statistical software (Minitab R12), as shown in Table 7. The results showed that there is an importance of displacement ductility with a thickness change from 3.34mm to 2.00mm, as well as with column lengths. The best stiffness importance was obtained in terms of changing tube thickness with a column length of 1445mm. Additionally, the analysis revealed a significant impact on displacement ductility due to a change in column length from 1450 mm to 2900 mm, resulting from the thickness of the column tube being 3.34 mm and 2.00 mm, respectively. The stiffness is insignificant in the case of a change in column length with tube thickness.

Table 7 Statistical Evaluation for the Displacement Ductility and Stiffness of CFST Frames.

Independent variable	Dependent variable	P-value
Tube thickness (column length 1445 mm)	Dis.ductility	0.041
Tube thickness (column length 2175 mm)	Dis.ductility	0.044
Tube thickness (column length 2900 mm)	Dis.ductility	0.048
Tube thickness (column length 1445 mm)	Stiffness	0.046
Tube thickness (column length 2175 mm)	Stiffness	0.053
Tube thickness (column length 2900 mm)	Stiffness	0.333
Column length (tube thickness 3.34mm)	Dis.ductility	0.045
Column length (tube thickness 2.67mm)	Dis.ductility	0.291
Column length (tube thickness 2.0mm)	Dis.ductility	0.031
Column length (tube thickness 3.34mm)	Stiffness	0.313
Column length (tube thickness 2.67mm)	Stiffness	0.333
Column length (tube thickness 2.0mm)	Stiffness	0.361

13.CONCLUSIONS

This study investigated the structural performance of CFST frames, which are composed of steel beams and CFST columns. To evaluate the frames' structural behavior, FE models were simulated using ANSYS software. To simulate the actual situation, an axial load was applied to the CFST columns while applying lateral forces up to failure. The conclusions that could be reached are listed below:

- The CFST frames showed the same failure modes. Plastic hinges started at the bottom and top of the CFST columns. There were no cracks in the filled concrete. Maximum stresses were observed at the base plate-CFST column and the steel beam-CFST column, with values of 381.46 and 386.63 MPa, respectively, indicating the development of a plastic hinge.
- The length and thickness of the steel tube in the CFST column both affected the ductility of the CFST frame. When the steel tube thickness was between 2.00 mm and 3.34 mm, ductility increased by approximately 2.9%. When the column length was between 1450 and 2900 mm, the improvement was approximately 1.25%.
- With a steel thickness of 3.34 mm, the CFST columns exhibited noticeably high stiffness; however, when the tube thickness was decreased, the stiffness also dropped. The force-displacement curves show this behavior. The CFST column's stiffness decreased as its length increased.
- The strengths of CFST frames with steel tube t = 3.34 mm and length L = 1450 mm, compared to CFST frames with L = 2175 mm and L = 2900 mm at ultimate strength, were 1.30 and 1.40, respectively.
- Statistical analysis revealed that increasing the length of the column with a small steel tube thickness, i.e., less than 2.67mm, insignificantly impacted the frame's ductility. On the other hand, increasing the column's length negatively impacted the frame's hardness in the case of a small steel tube thickness, i.e., less than 2.67mm.

ACKNOWLEDGEMENTS

The authors are grateful for the academic support provided for this research by the Civil Engineering Department, College of Engineering, University of Thi-Qar and Tikrit University. The research has been entirely funded by the author.

REFERENCES

[1] Shams M, Saadeghvaziri MA. **State of the Art of Concrete-Filled Steel Tubular Columns**. *Structural Journal* 1997; **94**(5): 558–571.

[2] Sahib HA, Al-Asadi AK. **Prediction of Shear Strength of CFRP-Strengthened Reinforced Recycled Aggregate Concrete Beams Using Various Strengthening Methods**. *Przegląd Naukowy Inżynieria i Kształtowanie Środowiska* 2022; **31**(4): 145–161.

[3] Hu HT, Huang CS, Wu MH, Wu YM. **Nonlinear Analysis of Axially Loaded Concrete-Filled Tube Columns with Confinement Effect**. *Journal of Structural Engineering* 2003; **129**(10): 1322–1329.

[4] Han LH, Yao GH, Tao Z. **Performance of Concrete-Filled Thin-Walled Steel Tubes Under Pure Torsion**. *Thin-Walled Structures* 2007; **45**(1): 24–36.

[5] Han LH, Wang WD, Tao Z. **Performance of Circular CFST Column to Steel Beam Frames Under Lateral Cyclic Loading**. *Journal of Constructional Steel Research* 2011; **67**(5): 876–890.

[6] Ding FX, Yin GA, Jiang LZ, Bai Y. **Composite Frame of Circular CFST Column to Steel-Concrete Composite Beam Under Lateral Cyclic Loading**. *Thin-Walled Structures* 2018; **122**: 137–146.

[7] Ahmed AD, Güneyisi E. **Lateral Response of Double Skin Tubular Column to Steel Beam Composite Frames**. *Turkish Journal of Engineering* 2022; **6**(1): 16–25.

[8] Ahmed AD, Güneyisi EM. **Structural Performance of Frames with Concrete-Filled Steel Tubular Columns and Steel Beams: Finite Element Approach**. *Advanced Composites Letters* 2019; **28**: 2633366X19894593.

[9] Thompson MK, Thompson JM. **ANSYS Mechanical APDL for Finite Element Analysis**. Butterworth-Heinemann; 2017.

[10] American Institute of Steel Construction (AISC). **Load and Resistance Factor Design Specification for Structural Steel Buildings**. AISC, Chicago, IL, USA; 1999.

[11] ACI Committee 318. **Building Code Requirements for Structural Concrete (ACI 318-05) and Commentary (ACI 318R-05)**. American Concrete Institute; 2005.

[12] Dawood MH, Al-Asadi AK. **Mechanical Properties and Flexural Behaviour of Reinforced Concrete Beams Containing Recycled Concrete Aggregate**. *Scientific Review Engineering and Environmental Studies (SREES)* 2022; **31**(4): 259–269.

[13] Issa AS, Al-Asadi AK. **Mechanical Properties of Lightweight Expanded Clay Aggregate (LECA) Concrete**. *Przegląd Naukowy Inżynieria i Kształtowanie Środowiska* 2022; **31**(3): 112–126.

[14] Elwi AA, Murray DW. **A 3D Hypoelastic Concrete Constitutive Relationship**. *Journal of the Engineering Mechanics Division* 1979; **105**(4): 623–641.

[15] Musthafa L, Rani S, KK S. **Study of Material Property of Concrete Filled Steel Tubular Columns**. *International Journal of Engineering Research & Technology* 2016; **5**(5): 504–508.

[16] Richart FE, Brandtzæg A, Brown RL. **A Study of the Failure of Concrete Under Combined Compressive Stresses**. University of Illinois Engineering Experiment Station Bulletin; No. 185; 1928.